HOKKAIDO UNIVERSITY

Title	Polyphosphate accumulation is driven by transcriptome alterations that lead to near-synchronous and near-equivalent uptake of inorganic cations in an arbuscular mycorrhizal fungus
Author(s)	Kikuchi, Yusuke; Hijikata, Nowaki; Yokoyama, Kaede; Ohtomo, Ryo; Handa, Yoshihiro; Kawaguchi, Masayoshi; Saito, Katsuharu; Ezawa, Tatsuhiro
Citation	New Phytologist, 204(3), 638-649 https://doi.org/10.1111/nph.12937
Issue Date	2014-11
Doc URL	http://hdl.handle.net/2115/58046
Rights	The definitive version is available at www.blackwellsynergy.com
Type	article (author version)
File Information	Kikuchi_NPH.pdf

Instructions for use

Hokkaido University Collection of Scholarly and Academic Papers : HUSCAP

New Phytologist

Article acceptance date: 11 June 2014

DOI: 10.1111/nph.12937

Title: Polyphosphate accumulation is driven by transcriptome alterations that lead to near-synchronous and -equivalent uptake of inorganic cations in an arbuscular mycorrhizal fungus

Authors: Yusuke Kikuchi[1], Nowaki Hijikata[1], Kaede Yokoyama[1], Ryo Ohtomo[2], Yoshihiro Handa[3], Masayoshi Kawaguchi[3], Katsuharu Saito[4], and Tatsuhiro Ezawa[1]*

Address: [1]Graduate School of Agriculture, Hokkaido University, Sapporo 060-8589, [2] National Agriculture and Food Research Organization, Hokkaido Agricultural Research Center, Sapporo 062-8555, [3]Division of Symbiotic Systems, National Institute for Basic Biology, Okazaki 444-8585, and [4]Faculty of Agriculture, Shinshu University, Minamiminowa 399-4598, Japan.

***Author for correspondence:**

Tatsuhiro Ezawa

Graduate school of Agriculture, Hokkaido University, Sapporo, Hokkaido 060-8589 Japan (tell & fax +81-11-857-9732; e-mail tatsu@res.agr.hokudai.ac.jp).

Summary

- Arbuscular mycorrhizal (AM) fungi accumulate a massive amount of phosphate as polyphosphate to deliver to the host, but the physiological and molecular mechanisms underlying have yet to be elucidated. In the present study, the dynamics of cationic components during polyphosphate accumulation were investigated in conjunction with transcriptome analysis.
- *Rhizophagus* sp. HR1 was grown with *Lotus japonicus* under phosphorus-deficient conditions, and extraradical mycelia were harvested after phosphate application at prescribed intervals. Levels of polyphosphate, inorganic cations, and amino acids were measured, and RNA-Seq was performed on the Illumina platform.
- Phosphate application triggered not only polyphosphate accumulation but also near-synchronous and -equivalent uptake of Na^+, K^+, Ca^{2+}, and Mg^{2+}, whereas no distinct changes in the levels of amino acids were observed. During polyphosphate accumulation, genes responsible for mineral uptake, phosphate and nitrogen metabolisms, and maintenance of cellular homeostasis were up-regulated.
- The results suggest that the inorganic cations play a major role in neutralizing negative charge of polyphosphate, and these processes are achieved by the orchestrated regulation of gene expression. Our findings for the first time provide a global picture of the cellular responses to increased phosphate availability, which is the initial process of nutrient delivery in the associations.

Key words: arbuscular mycorrhizal fungi, inorganic cation, polyphosphate, symbiosis, transcriptome.

Introduction

Arbuscular mycorrhizal (AM) fungi form symbiotic associations with most land plants and promote growth of the host plants through enhanced uptakes of mineral nutrients, particularly phosphorus (Smith & Read, 2008). The fungi take up inorganic phosphate (Pi) from the soil and accumulate it as polyphosphate (polyP) that is likely to be involved in the long-distance translocation of Pi through hyphae (Hijikata *et al.*, 2010). PolyP is a linear chain of three to hundreds Pi-residues linked by high-energy phosphoanhydride bonds (Kornberg *et al*., 1999). AM fungi grown under P deficient conditions are capable of accumulating a massive amount of polyP, up to 64% of total cellular P, within several hours in response to increased Pi availability (Hijikata *et al.*, 2010), which is considered to be an adaptive trait commonly evolved in microorganisms to prepare P deficiency, namely 'polyP-overcompensation (overplus)' (Harold, 1966). In natural ecosystems, patches of nutrients are associated with decomposing organic residues, e.g., leaf litter and dead bodies of animals (reviewed in Tibbett, 2000). PolyP overplus, therefore, would be an important trait that allows AM fungi to capture Pi efficiently from such nutrient patches, which consequently has a large impact on nutrient acquisition strategies of the plants.

Fungi take up Pi mainly through the high-affinity H^+/Pi symporter that was first identified in *Saccharomyces cerevisiae* as *PHO84* (Bun-Ya *et al*., 1991). The symporter also plays a significant role in Pi uptake in AM fungi (Harrison & Van Buuren, 1995). In contrast to extensive studies on the H^+/Pi symporters, the enzyme responsible for polyP biosynthesis in eukaryotic microorganisms has only recently been identified in *S. cerevisiae*; a complex of vacuolar transporter chaperons (VTC complex) at the vacuolar membrane polymerizes the γ-phosphate of ATP supplied in the cytosol and releases the polymer into the vacuole (Hothorn *et al*., 2009). It is highly likely that AM fungi synthesize polyP also via the VTC

complex (Tisserant *et al*., 2012) using ATP as substrate (Tani *et al*., 2009) (Fig. 1). In the newly released genome sequence of the model AM fungus *Rhizophagus irregularis*, approximately 23,000 genes were predicted and expressed in spores and/or intraradical mycelia (Tisserant *et al*., 2013). Transcriptional regulation of the genes in response to environmental changes, however, has yet to be elucidated. In particular, information about responses to increased Pi availability in extraradical mycelia is of great interest, but still fragmented.

PolyP is a polyanionic compound, and fully dissociated polyP has one negative charge per Pi residue in addition to the two extra charges of terminal residues (Fig. S1 in Supporting Information). PolyP overplus, therefore, should result in accumulation of a large amount of negative charge in the cell, suggesting that there would be a regulatory mechanism for maintaining charge neutrality of the cell. Inorganic cations and basic (cationic) amino acids are likely to be potential counter ions for polyP (Fig. 1). In four ectomycorrhizal fungi (Bücking & Heyser, 1999) and an AM fungus (Bücking & Shachar-Hill, 2005) energy dispersed X-ray spectroscopic analysis revealed that various di- and monovalent cations, magnesium (Mg), calcium (Ca), potassium (K), and sodium (Na) were colocalized with P in their vacuoles. In *Neurospora crassa* these four cations were also detected in the isolated vacuoles in which polyP was accumulated (Cramer & Davis, 1984). On the other hand, arginine that has one basic side group in the molecule is the most abundant amino acid in AM fungi (Johansen *et al.*, 1996; Jin *et al.*, 2005) and a translocation form of nitrogen towards the plants (Govindarajulu *et al*., 2005), leading to the idea that arginine would be associated with polyP and cotranslocated (Bago *et al.*, 2001). *In vivo* ionic interactions between basic amino acid and polyP, however, have been controversial; polyP degradation resulted in the release of an equivalent amount of arginine from the vacuole in *S. cerevisiae* (Dürr *et al.*, 1979), whereas in *N. crassa* basic amino acids were retained in the vacuoles even after most polyP

was degraded (Cramer & Davis, 1984). Accordingly, elucidation of quantitative relationship between polyP and these cationic components is necessary for understanding the regulatory mechanism of charge neutrality during polyP accumulation.

RNA-Seq, the high-throughput next-generation sequencing technology for transcriptome, provides a largely unbiased method to explore comprehensive gene structure and expression profile. On the other hand, we have developed a mass production system for extraradical mycelia of AM fungi, which enabled us to study polyP biosynthesis (Tani *et al*., 2009) and dynamics (Hijikata *et al*., 2010). In the present study, the mass production system was applied for quantitative analysis of cationic components and also for preparation of high-quality RNA for RNA-Seq toward a comprehensive understanding of the cellular and molecular processes involved in polyP overplus in AM fungi.

Materials and methods

Fungal material

The AM fungus *Rhizophagus* sp. strain HR1 (MAFF520076) has been maintained with sand culture in a greenhouse, and GenBank accession numbers of the small- and large-subunit ribosomal RNA gene (SSU rDNA and LSU rDNA) sequences are AB220171 and AB370889, respectively. The SSU rDNA sequence showed high-similarity to *R. manihotis* (Y17648), *R. clarus* (AJ852597), and *R. intraradices* (FR750209 and EU232660), while the LSU rDNA sequence showed high-similarity to *R. intraradices* (DQ469108 and FJ235569) and *R. irregularis* (FR750084 and FR750070). This strain produces many hyphae with few spores during vegetative growth of the host plant and thus suitable for physiological study.

Culture conditions

Lotus japonicus L. cv. Miyakojima MG-20 (National Bioresource Project Legume Base, http://www.legumebase.agr.miyazaki-u.ac.jp/index.jsp) was sown on a moistened filter paper in a Petri dish and germinated at 25°C for 2 days in the dark. Four seedlings were transplanted to mycorrhizal compartment (MC) of the mesh bag culture system in a 120 ml plastic pot (6 cm in diam) and inoculated with *Rhizophagus* sp. HR1 at 500 spores pot^{-1}. The mesh bag system consisted of the MC and hyphal compartment (HC) that were separated by a cone-shaped 37-μm nylon mesh bag (Nippon Rikagaku Kikai) of which volume was 26 ml (Fig. S2). The pore size of the nylon mesh was small enough to prevent *L. japonicus* roots from passing but large enough to allow AM fungal hyphae to pass through. In the previous study (Hijikata *et al*., 2010) a P-diffusion barrier between the compartments was inserted, but not in the present study, because diffusion of a minimum amount of Pi from the HC to the MC across the nylon mesh did not affect polyP accumulation in extraradical mycelia in the HC at least within 24 h (data not shown). Media in the two compartments were prepared as follows: river sand was washed with tap water by decantation, dried, separated by stainless sieves into two fractions of which particle size distributions were 0.1 – 3 and 1 – 3 mm for the MC and HC, respectively, rinsed with deionized water (DIW), and autoclaved. The sand in the HC (1 – 3 mm) enabled rapid and efficient separation of mycelia from sand particles, which was essential for element analysis and preparation of high-quality RNA, while that in the MC (0.1 – 3 mm) was optimized for plant growth. The seedlings were grown in a growth chamber (16-h photoperiod and 25°C with photosynthetic photon flux density at 150 μmol m^{-2} s^{-1}) and thinned to 2 plants pot^{-1} after one week. The plants received DIW every other day for the first week, low-P nutrient solution (4 mM NH_4NO_3, 1 mM K_2SO_4, 0.75 mM $MgSO_4$, 2 mM $CaCl_2$, 50 μM Fe-Na-EDTA, 50 μM KH_2PO_4, pH 5.4) for the second to sixth week, and

then non-P nutrient solution (KH_2PO_4 was withheld from the low-P nutrient solution) for the seventh week in a sufficient amount until the solution flowed out from the drain. At the beginning of eighth week, a 1 mM KH_2PO_4 (pH 4.8) solution was applied to the HC using a pipette in a sufficient amount until the solution flowed out from the drain (*ca*. 15 ml). The Pi solution was washed out with DIW in a sufficient amount 1 h after Pi application, and then extraradical mycelia in the HC were harvested from two pots together by wet sieving at prescribed time intervals and combined as one sample. Immediately after harvest, all visible sand particles adhering to the mycelia were removed under a dissecting microscope with forceps as quickly as possible, and the mycelia were frozen in liquid nitrogen and stored at –80°C. At all time points, 6 pots were harvested to obtain three replicates (n =3).

Polyphosphate, inorganic cation, and amino acid analyses

The frozen mycelial sample (approx. 20 – 40 mg FW per sample) was ground on an ice-cooled mortar and pestle with a 30-fold volume (v/w) of 10 mM Tris-HCl buffer (pH 8.0). Subsamples for protein (10 µl) and amino acid (200 µl) analyses were taken from the slurry and stored at -30°C. Then 300 µl of the slurry was mixed with 219 mg powdered urea (the final concentration of urea was 8 M) and centrifuged at 18,000 × g for 10 min at 10°C. For inorganic cation analysis, 250 µl of supernatant was taken and stored at –30˚C. For polyP analysis, 75 µl of supernatant was desalted immediately after centrifugation with Micro Bio-Spin P-6 gel filtration spin column (Bio-Rad Laboratories) pretreated with TE buffer (10 mM Tris-HCl, 1 mM EDTA, pH 8.0), and polyP concentration was determined by the reverse reaction of polyP kinase (PPK) purified from PPK-overexpressing *E. coli* (Ault-Riché *et al.*, 1998) as described previously (Ezawa *et al.*, 2003). Concentration of polyP was expressed in terms of electric charge mol (mol_c) of Pi-residues per unit protein. In this calculation one

negative charge per residue was assumed i.e. a $polyP_n$ molecule possesses n charges (where n represents no. of Pi-residue), although a fully dissociated $polyP_n$ theoretically possesses n+2 charges of which the two extra charges are of terminal residues at both ends. This is because i) the terminal charges might be negligible if chain-length of polyP in AM fungi is more than 300 as estimated in Ezawa *et al*. (2003) and ii) accurate estimation of chain-length distribution of polyP is technically difficult. For inorganic cation analysis, the stored supernatant (250 µl) was heated in 2.0 ml of 15% (v/v) sulfuric acid at 105˚C for 1 h to evaporate water (until sulfuric acid was concentrated) and then digested at 105°C for 5 h by adding 0.1 ml hydrogen peroxide four times at 1 h intervals as an oxidant. Concentrations of sodium (Na^+), potassium (K^+), calcium (Ca^{2+}), magnesium (Mg^{2+}), ferric (Fe^{2+}), zinc (Zn^{2+}), aluminum (Al^{3+}), copper (Cu^{2+}), nickel (Ni^{2+}), and manganese (Mn^{2+}) ions in the digests were determined by an inductively-coupled plasma mass spectrometer (ELAN DRC II, PerkinElmer) using the ICP multi-element standard solution IV (Merck) as standard. Concentrations of the cations were given in terms of electric charge mol (mol_c) per unit protein. For free amino acids analysis, the slurry (200 µl) was mixed with an equal volume of 20% (w/v) trichloroacetic acid, kept for 2 h at 4°C, and centrifuged at 18,000 × *g* for 15 min at 4°C, and then trichloroacetic acid was extracted three times with ice-cooled 500 µl water-saturated dimethyl ether. After air-drying for 1 h, 160 µl of the solution was mixed with 40 µl 0.1 M hydrochloric acid, filtrated through the 0.45 µm Millex-LH PTFE membrane filter (Millipore), and introduced to an amino acid analyzer (L-8500, Hitachi). Protein concentration was determined with *DC* Protein Assay Kit (Bio-Rad Laboratories) according to the manufacturer's instructions using bovine serum albumin as standard. For conversion of concentration data (per unit protein) to those on the basis of unit dry weight, or vice versa, the conversion coefficients 13 – 18 mg protein g^{-1} FW with 80% (w/w) water content, which were determined using several lots of mycelia, were used. StatView software

(SAS Institute Inc.) was employed for analysis of variance (ANOVA) and Tukey-Kramer post-hoc test.

RNA-Seq and expression analysis

Total RNA was extracted from the frozen mycelia (20 to 40 mg FW) obtained at time zero and 4 h after Pi application with RNeasy Plant Mini Kit (Qiagen), followed by RNase-free DNase I (Qiagen) treatment (n = 3 for each time point). Sequencing libraries were constructed using 500 ng of total RNA with TruSeq RNA Sample Prep kit (Illumina) following the manufacturer's instructions. Paired-end 101 bp × 2 sequencing were performed with HiSeq2000 (Illumina). Raw sequence data were deposited in DDBJ Sequence Read Archive under accession number DRA001877. High-quality reads of which > 90% bases showed Phred quality scores > 20 were extracted and assembled with Trinity (Grabherr *et al*., 2011).

The assembled sequences (contigs) were queried against the predicted gene models (Gloin1_all_transcripts_20120510.nt.fasta) and expression sequence tags (ESTs) (Gloin1_ESTs_20120510_Combest_RNA_and_EST_contigs.fasta) of *R. irregularis* DAOM 181602 in DOE Joint Genome Institute (http://genome.jgi.doe.gov/Gloin1/Gloin1.home.html) as well as against GenBank nucleotide collection with the BLASTN algorithm at an e-value cutoff of 10^{-5}, and then contigs that showed higher similarity (i.e. a lower e-value and a higher bit score) to the sequences in the *R. irregularis* genome database than those in GenBank were defined to be of *Rhizophagus* sp. HR1 origin. Open reading frames (ORFs) of 50 or longer amino acid residues were predicted and extracted from the contigs by using the utility program of Trinity (transcripts_to_best_scoring_ORFs.pl) and clustered using CD-HIT-EST with a 95% sequence identity cutoff, and then the longest ORFs were selected

as representatives from each cluster to minimize duplication of putative splice variants, polymorphisms, and fragmented (frameshifted) ORFs in the predicted gene set (W. Li & Godzik, 2006). Putative functions of the ORFs were assigned in reference to the *Saccharomyces cerevisiae* protein database (orf_trans.fasta) in *Saccharomyces* Genome Database (SGD) (http://www.yeastgenome.org/) and the *Neurospora crassa* protein database (neurospora_crassa_or74a__finished__10_proteins.fasta) at Broad Institute (http://www.broadinstitute.org/annotation/genome/neurospora/MultiHome.html) by the BLASTP algorithm at an e-value cutoff of 10^{-5}. The gene ontology (GO) functional classes were assigned in reference to those of *S. cerevisiae* (go_terms.tab) in SGD and *N. crassa* (go_for_nc12.tsv) at Broad Institute.

Expression levels of transcripts were estimated based on the number of reads that were uniquely mapped to the corresponding ORF sequences using Burrows-Wheeler Aligner's Smith-Waterman algorithm with default parameters, in which five nucleotide-mismatches were allowed in the alignment between a read (101 bp) and the ORF sequence (H. Li & Durbin, 2010). The reads that were mapped to multiple locations in an ORF or to multiple ORFs were discarded using SAMtools (H. Li *et al*., 2009). The raw read counts were normalized with the iDEGES/edgeR method (Sun *et al*., 2013), and pairwise comparisons of digital gene expression between the time points were conducted with the edgeR program in R (Robinson *et al*., 2010). The false discovery rate (FDR) adjustments (Benjamini & Hochberg, 1995) were applied to correct for multiple testing, and differentially expressed genes were identified with an FDR threshold of 0.05. To identify GO terms in which up- or down-regulated genes were overrepresented, the enrichment analysis tool in Blast2GO program (Conesa *et al*., 2005) was employed with an FDR threshold of 0.05.

Quantitative RT-PCR

Total RNA (500 ng) was reverse-transcribed with the mixture of random and oligo dT primers using PrimeScript RT Master Mix Kit (Takara), and quantitative PCR was performed using SYBR Premix Ex Taq II (Takara) with LightCycler (Roche) according to the manufacturer's instructions with the thermal cycle program of 95°C for 30 s and 40 cycles of 95°C for 5 s and 60°C for 20 s. Target genes and corresponding primers are listed in Table S1. The levels of transcripts were evaluated by the relative standard curve method using an α-tubulin gene as internal standard.

Results

Dynamics of inorganic cations and amino acids during polyphosphate accumulation

PolyP rapidly increased from 0.1 to 18.9 $\mu mol_c\ mg^{-1}$ protein 4 h after Pi application (Fig. 2a). During polyP accumulation, levels of Na^+ and K^+ remained constant until 2 h after Pi application and then increased to 9.5 and 5.7 $\mu mol_c\ mg^{-1}$ protein, respectively, 4 h after Pi application (Fig. 2b), and those of Ca^{2+} and Mg^{2+} also remained constant until 2 h after Pi application and increased to 7.4 and 3.4 $\mu mol_c\ mg^{-1}$ protein, respectively, 4 h after Pi application (Fig. 2c). Levels of Fe^{2+} were an order of magnitude lower than those of the four major cations, and no significant change in the level was observed during polyP accumulation (Fig. S3). Concentrations of Zn^{2+}, Al^{3+}, Cu^{2+}, Ni^{2+}, and Mn^{2+} were two to several orders of magnitude lower than those of the four major cations, and no consistent results were obtained (data not shown). Arginine was the most abundant free amino acid, followed by asparagine, glutamic acid, and alanine (Tables S2), which accounted for 53 – 61, 13 – 15, 3 – 5, and 3 –

4% of total amino acid, respectively. No significant change in arginine level was observed during polyP accumulation (Fig. 2d). Asparagine levels were also constant during polyP accumulation, whereas glutamic acid and alanine levels were significantly decreased 1 and 3 h after Pi application, respectively. Levels of other amino acids and ammonium (NH_4^+) were less than one-twentieth of that of arginine and did not change during polyP accumulation, except for threonine, glutamine, and valine that were slightly decreased after Pi application. During polyP accumulation, cellular ATP levels were constant, and no significant perturbation in the level was observed (data not shown).

Dynamics of the four major cations during polyP accumulation were further investigated from 0 to 24 h after Pi application. PolyP increased from 1.5 to 14.3 $\mu mol_c\ mg^{-1}$ protein 4 h after Pi application and then decreased to the initial level 24 h after Pi application (Fig. 3a). Na^+ and K^+ increased from 1.1 to 4.2 $\mu mol_c\ mg^{-1}$ protein and from 0.4 to 1.8 $\mu mol_c\ mg^{-1}$ protein, respectively, 8 h after Pi application and then decreased to the initial levels 16 h after Pi application (Fig. 3b). Ca^{2+} and Mg^{2+} levels increased from 2.8 to 5.7 $\mu mol_c\ mg^{-1}$ protein and from 1.8 to 4.3 $\mu mol_c\ mg^{-1}$ protein, respectively, 8 h after Pi application and then decreased to the initial levels 24 h after Pi application (Fig. 3c). Net changes in total level of the four cations were compared with those in polyP level from time zero to 24 h after Pi application based on the data shown in Fig. 3: total levels of the cations increased and decreased near-synchronously with and -equivalently to the levels of polyP, although the total levels reached a maximum about 4 h later than those of polyP (Fig. 4). A net increase in the level ($\mu mol_c\ mg^{-1}$) from 0 to 8 h after Pi application was largest in Na^+ (3.1), followed by Ca^{2+} (2.9), Mg^{2+} (2.5), and K^+ (1.4).

RNA-Seq overview

The high-throughput sequencing produced a total of 183 millions of 101 bp paired-end reads (Table S3). After filtering, 143 millions of high-quality reads were obtained and assembled into 319,615 contigs to which 57.3% of the filtered reads were uniquely mapped back to the contigs, that is, 43.1% of the reads were mapped to multiple locations in a contig or multiple contigs (Fig. S4 and Table S4). Among them, 47,366 contigs showed higher similarities to the predicted gene models and ESTs of *R. irregularis* than to those of other organisms in GenBank nucleotide collection, suggesting that they are likely to be of *Rhizophagus* sp. HR1 origin. To these contigs, 43.1% of the filtered reads (i.e. 75.2% of the uniquely mapped reads) were mapped. Whereas only 14.2% of the filtered reads were mapped to the rest of the contigs (272,249 contigs) that would include not only misassembled contigs and contamination from other organisms but also transcripts of *Rhizophagus* sp. HR1 genes that are not conserved between *R. irregularis*. From the 47,366 putative *Rhizophagus* sp. HR1 transcripts, a total of 19,144 ORFs (i.e. protein-coding genes) were predicted, to which 31.6 million reads (22.1% of the reads) were uniquely mapped and thus were subjected to subsequent expression analysis. With reference to either the *S. cerevisiae* or *N. crassa* databases, 7,876 out the 19,144 predicted genes (41.1%) could be functionally annotated. Although possibility of the presence of splice variants/polymorphisms in the predicted gene set cannot be absolutely excluded, the number of predicted genes in our RNA-Seq is comparable to that of the expressed genes (16,000 – 18,000) in *Rhizophagus* spp. (Tisserant *et al*., 2013), suggesting that variants/polymorphisms are minimum within the predicted genes and also that the gene set provides a reasonable coverage of transcriptome in extraradical mycelia of *Rhizophagus* sp. HR1. The sequences of putative *Rhizophagus* sp. HR1 transcripts and predicted genes (ORFs) are available at http://www.agr.hokudai.ac.jp/botagr/rhizo/RhizoCont/Download.html.

Purity of the fungal material obtained from the open pot culture was evaluated based

on proportions of reads mapped to ribosomal RNA gene (rDNA) of other microorganisms that were contaminated in the fractions. Although about 45.0 millions of the filtered reads were mapped to contigs similar to rDNA of various organisms, 94.4% of these reads (42.4 million reads) were mapped to 7 contigs (including variants in the divergent domains) that showed the highest similarity to the rDNAs of *Rhizophagus* sp. HR1 and its close relative (Fig. S5 and Table S5). These observations suggested that contamination of transcripts from other organisms was minimum in the RNA-Seq analysis.

Dynamics of gene expression during polyphosphate accumulation

Among the 19,144 predicted genes, significant changes in expression level during polyP accumulation were observed in 2,332 genes; 1,582 and 750 were up- and down-regulated, respectively, 4 h after Pi application (Fig. S6 and Table S6). To evaluate validity of these results, qRT-PCR was conducted using the same RNA extracts on nine genes responsible for Pi uptake, polyP biosynthesis, and cation transport (listed in Table S1). The differential expression levels (fold change in response to Pi application) of the genes observed in the RNA-Seq analysis were significantly correlated with those determined by qRT-PCR (r = 0.906, $P < 0.001$), validating the results of RNA-Seq analysis (Fig. S7).

In 155 GO terms involved in Pi transport, cation transport, polyP metabolism, arginine metabolism, cellular pH regulation, and ribonucleotide metabolism up-regulated genes were overrepresented (Table S7). Whereas down-regulated genes were overrepresented in 18 GO terms involved mainly in antioxidant reactions and nitrate assimilation/metabolism (Table S8). Genes assigned to the GO terms involved in ATP/energy generation pathways, e.g., glycolysis (GO:0006096), pentose phosphate shunt (GO:0006098), TCA cycle (GO:0006099), β-oxidation (GO:0006635), and oxidative phosphorylation (GO:0006119),

were generally unresponsive to Pi application, or slightly down-regulated (data not shown), except that *AAC* that encodes ADP/ATP carrier of the mitochondrial inner membrane (ORF ID Rh118606 in Table S6) was up-regulated.

For further analysis, detailed profiling of the genes in these GO terms in addition to those that showed significant changes in expression level was conducted with particular emphasis on the dynamics of cation and amino acid during polyP accumulation.

Phosphate uptake and polyphosphate metabolism: Pi application significantly increased expression of the genes responsible for Pi uptake across the plasma membrane: four out of six H^+/Pi symporter genes (*PHO84*) and two Na^+/Pi symporter genes (*PHO89*) (Fig. 5 and Table S9). Two out of four plasma membrane (P)-type H^+-ATPase genes and all four Na^+-ATPase genes that are responsible for driving the H^+/Pi- and Na^+/Pi-symporters, respectively, were also up-regulated by Pi application. Expression levels of H^+/Na^+ antiporter genes (*NHA*) responsible for Na^+ extrusion across the plasma membrane were also increased by Pi application. Expression of *VTC1* and *VTC4* responsible for polyP biosynthesis dramatically increased by Pi application, and in addition, an endopolyphosphatase gene (*PPN*) and a vacuolar membrane (V)-type Pi exporter gene (*PHO91*) were also up-regulated by Pi application.

Cation transport: Various genes responsible for inorganic cation uptake across the plasma membrane were up-regulated by Pi application: K^+ transporter genes (*KTR*), Mg^{2+} transporter genes (*ALR*), a Fe^{3+} permease gene (*FTR*), a Zn^{2+} transporter gene (*ZRT*), and a divalent metal ion transporter genes (*SMF*), whereas no significant changes in expression levels of a Ca^{2+} channel (*CCH*) and a Ni^{2+} transporter (*NTR*) genes were observed. Genes responsible for inorganic cation transport across the vacuole membrane, a H^+/monovalent cation antiporter gene (*VNX*), H^+/Ca^{2+} antiporter genes (*VCX*), a Fe^{2+}/Mn^{2+} transporter gene (*CCC*), a Zn^{2+} transporter gene (*ZRC*), a Zn^{2+} exporter gene (*ZRE*), a Ca^{2+}-ATPase gene, were up-regulated

in response to Pi application. Expression of several genes encoding the subunits of V-type H^+-ATPase that drives ion transport across vacuolar membrane were also increased by Pi application. No significant change in the expression level of V-type Cu^{2+} transporter gene (*CTR*) was observed.

Nitrogen uptake and arginine metabolism: Pi application generally reduced expression of the genes involved in nitrate assimilation: two NO_3^- transporter genes (*NRT*), one of nine NO_3^- reductase genes (*NAR*) and two of five NO_2^- reductase genes (*NIR*) (Fig. 6 and Table S10). In contrast, Pi application generally up-regulated the genes involved in NH_4^+ uptake, nitrogen assimilation, and arginine biosynthesis (urea cycle): one of four NH_4^+ permease genes (*MEP*) of which transcripts were most abundant among the four, two glutamine synthetase genes (*GS*), one of two glutamate synthase genes (*GOGAT*), a carbamoyl phosphate synthetase gene (*CPS*), an acetylglutamate kinase and N-acetyl-γ-glutamyl-phosphate reductase (*AGK*/*AGPR*), an acetylornithine aminotransferase gene (*AOAT*), an ornithine carbamoyltransferase gene (*OCT*), an argininosuccinate synthetase gene (*ASS*), and an argininosuccinate lyase gene (*ASL*). Only one of four *MEP* and an ornithine acetyltransferase gene (*OAT*) were down-regulated after Pi application. Expression of an arginase gene (*ARG*) and an ornithine transaminase gene (*OTA*) responsible for arginine degradation was also increased by Pi application. Interestingly, both a V-type basic amino acid transporter gene (*VBA*) involved in sequestration into the vacuoles and two V-type basic amino acid exporter genes (*RTC*) involved in release from the vacuoles were up-regulated by Pi application.

Discussion

The present study for the first time demonstrates a global picture of transport and metabolic

processes during polyP accumulation in an AM fungus both at the physiological and molecular levels. The application of 1 mM Pi to Pi-starved hyphae induced polyP overplus in the fungus. Although such high-concentration of Pi may rarely occur in natural soils, this approach enhanced cellular responses to increased Pi availability and thus enabled us to clarify the orchestrated cellular processes involved in Pi acquisition in the symbiotic phase of the fungus. The micro-scale element/amino acid analyses in conjunction with the transcriptome analysis revealed that polyP overplus was concurrent with rapid uptake of inorganic cations, but not with drastic changes in cationic amino acid levels, during which not only the genes responsible for Pi uptake and polyP biosynthesis but also those responsible for inorganic cation transport were up-regulated. These results suggest that inorganic cations play a significant role in maintaining cellular homeostasis during polyP accumulation in the fungus.

Transport and metabolic processes responsible for polyphosphate accumulation

The comparative transcriptome analysis revealed that Pi application to Pi-starved hyphae induced the expression of the genes encoding Pi symporters, P-type ATPases, and polyP polymerase (VTC complex). Interestingly, *PPN*, vacuolar endopolyphosphatase responsible for polyP hydrolysis (Kumble & Kornberg, 1996), and *PHO91*, a V-type Pi exporter that releases Pi from the vacuoles (Hürlimann *et al*., 2007), were also up-regulated, supporting the idea that polyP is dynamically turning over during the accumulation and translocation (Ezawa *et al*., 2001). Although we initially expected that genes involved in the ATP/energy generation pathways would also be up-regulated to supply ATP to polyP biosynthesis, most of the genes involved in the pathway were unresponsive to Pi application. However, the increased expression level of *AAC*, a mitochondrial ADP/ATP carrier gene that exchanges

cytosolic ADP for mitochondrial ATP (Lowson & Douglas 1988), suggests that ATP export from mitochondria to the cytosol was increased during polyP accumulation. Given that no perturbation in cellular ATP level was observed during polyP accumulation, the ATP/energy generation pathways are likely to be fully capable of covering the increased ATP demand for polyP overplus without up-regulation of the genes.

The comparative transcriptome analysis also unveiled a complex regulatory mechanism underlying Pi uptake through the two types of high-affinity Pi transporter, H^+- and Na^+-dependent symporters. In contrast to H^+-dependent Pi uptake, less attention has been paid to Na^+-dependent Pi uptake in AM fungi (Ezawa *et al*., 2002). The pathway, however, is common in mammals (Collins *et al*., 2004), protozoa (Dick *et al*., 2012), and fungi (Versaw & Metzenberg, 1995; Zvyagilskaya & Persson, 2003). In AM fungi the expression of the gene has only recently been described (Tisserant, *et al*., 2012). A fungal Na^+/Pi symporter was first identified as *PHO4* in *N. crassa* (Versaw & Metzenberg, 1995), and then the yeast homologue *PHO89* was characterized in detail (Martinez & Persson, 1998; Zvyagilskaya *et al*., 2008). The *PHO89* encodes a high-affinity Na^+/Pi symporter responsible for Na^+-coupled Pi transport with an alkaline pH optimum, which is driven by the electrochemical gradient of Na^+ across the plasma membrane generated by Na^+-ATPase (Zvyagilskaya *et al*., 2008). The expression of *PHO89* was significantly increased in response to Pi application in *Rhizophagus* sp. HR1, which was concurrent with the up-regulation of the Na^+-ATPase genes, indicating the significance of Na^+-dependent Pi uptake pathway in the Pi acquisition strategy of AM fungi. For the parallel driving of H^+- and Na^+-dependent pathways, it is likely that at least two types of H^+/Na^+ antiporter, in addition to the P- and V-type ATPases, are required; one is the P-type antiporter encoded by *NHA*, and the other is the V-type antiporter encoded by *VNX*, of which expression was up-regulated in response to Pi application. The former antiporter NHA extrudes Na^+ in exchange for H^+ across the plasmamembrane (Bañuelos *et al*.,

1998), whereas the latter antiporter VNX sequesters Na^+ into the vacuoles in exchange for H^+ (Cagnac *et al*., 2007). The coordinated expression of these genes may be responsible for the maintenance of pH/Na^+ homeostasis during polyP accumulation.

A moderate concentration of Pi (i.e. 320 μM) up-regulated the H^+/Pi symporter gene in Pi-starved extraradical mycelia of *R. irregularis in vitro* culture, although high-concentrations of Pi (>3 mM) down-regulated the expression at least within 24 h (Maldonado-Mendoza *et al*., 2001; Fiorilli *et al*., 2013). The detachment of mycelia from the roots, however, suppressed the expression even in the presence of 320 μM Pi, suggesting that the expression is regulated by the sink activity of the host rather than by external Pi (Fiorilli *et al*., 2013). Given that the host would receive Pi from the fungus at least 8 – 10 h after Pi application in our culture system (Hijikata *et al*., 2010), the sink activity was likely to be maintained 0 – 4 h after Pi application during which the transcript levels were assessed, and thus the expression of the symporter genes were maintained even in the presence of a high-concentration (1 mM) of Pi.

Roles of inorganic cations in polyphosphate accumulation

The time course quantitative analysis of cationic components revealed that Na^+, K^+, Ca^{2+}, and Mg^{2+} were taken up near-synchronously with and -equivalently to polyP, providing strong evidence that they play a major role in neutralization of negative charge of polyP in the fungal cell. Although subcellular localization of the increased cations has yet to be elucidated, it is highly likely that a large part of these cations were sequestered into the vacuoles where polyP was accumulated due to the following observations; i) the colocalization of these four cations with P in the vacuoles of *R. irregularis* has been observed previously (Bücking & Shachar-Hill, 2005) and ii) the genes encoding the V-type inorganic cation transporters were

up-regulated in response to Pi application.

The concentrations of polyP, K^+, and Ca^{2+} on the basis of protein (in Fig. 4) can be converted to those on the basis of dry weight for direct comparison with the data obtained previously ($\mu mol_c\ g^{-1}$ DW): polyP, 1,230-1,700; K^+, 370 – 512; Ca^{2+}, 480 – 666. Olsson *et al.* (2008) employed particle-induced X-ray emission analysis in conjunction with ion scanning transmission microscopy for the estimation of element contents in *R. irregularis* spores grown *in vitro*: P, 8,000; K, 2,800; Ca, 2,300 $\mu g\ g^{-1}$ DW, which correspond to 258, 72 and 116 $\mu mol_c\ g^{-1}$ DW, respectively. Absolute values are largely different between the two studies, probably because they were obtained in different tissue (spores and hyphae) grown under different conditions (*in vitro* and open pot culture). Nevertheless, P: K: Ca molar ratios are quite similar between the two studies; 10: 2.8: 4.5 in Olsson *et al.* (2008) and 10: 3.0: 3.9 in the present study. These observations suggest that the fungi selectively take up K^+ and Ca^{2+} (and probably also Na^+ and Mg^{2+}) to maintain charge neutrality in the cell, independent of availability of these cations in the environment (culture medium). This idea is indirectly supported by the following results; i) the net increase in K^+ during polyP accumulation was smallest among the four cations, even though Pi was applied in the form of potassium dihydrogen salt and ii) both Fe^{2+} and Na^+ were applied at 50 μM in the nutrient solution, but the levels of Fe^{2+} were unresponsive to polyP and less than an order of magnitude lower than those of Na^+, suggesting highly selective cation uptake in the fungi. Further experiments under various cation-availability conditions are necessary to confirm this idea.

The rapid decreases in polyP level from 4 h after Pi application suggests that polyP is highly mobile in the cell and thus readily translocated through hyphae towards the plant, as demonstrated previously (Hijikata, *et al.*, 2010). To maintain the mobility, maintaining solubility of polyP is essential, which is likely to be regulated by counter ions and pH in the vacuoles. MacDonald and Mazurek (1987) postulated that polyP has two dissociation

constants K_{a1} and K_{a2} and estimated the values by NMR based on the chemical shifts of protonated Pi-residue; in the presence of monovalent cation, pK_{a1} and pK_{a2} values of $polyP_{16}$ (polyP of 16 Pi-residues) were 5.0 – 5.7 and 6.2 – 6.5, respectively, whereas the addition of divalent cation to the solution significantly decreased the values to < 4.0 and < 4.5, respectively. Given that vacuolar pH of *R. irregularis* might be 5.5 – 6.0 and constant even after Pi application (Viereck *et al*., 2004), the presence of divalent cation in the vacuoles is likely to lead to dissociation of polyP, which would consequently maintain solubility of polyP.

At the initial phase of polyP accumulation (i.e. from 0 to 4 h after Pi application), however, the total cation levels were about 30% lower than those of polyP in terms of charge, implying that Pi uptake (and subsequent polyP synthesis) and cation uptake were transiently imbalanced in this phase. During the phase, it seems likely that a part of Pi-residues of polyP was temporally protonated, which was probably assisted through H^+ transport by V-type H^+-ATPases. Although solubility of partially (i.e. 30% of Pi-residues) protonated polyP has not been experimentally investigated, the fact that total P levels fluctuated in parallel with soluble (urea-extractable) polyP levels after Pi application (Hijikata *et al*., 2010) suggests that precipitation of polyP i.e. conversion of 'soluble polyP' to 'insoluble polyP' was unlikely to occur in this phase.

The synchronous decreases in the four major cations with polyP from 4 h after Pi application suggest that these cations were translocated in association with polyP towards the plant, at least to intraradical hyphae, although our experimental setup did not allow us to address the issue. There are many reports demonstrating that AM formation increased concentration of various cations in the host, e.g., Na (Tian *et al*., 2004), K (Huang *et al*., 1985), Mg (Giri & Mukerji, 2004), and Cu (X. L. Li *et al*., 1991), which indirectly suggest that metal cations are transferred from the fungi to the host. A direct answer to the question

whether cation transfer between the symbionts occurs would be obtained by using radioactive tracers (e.g., ^{65}Zn in Bürkert & Robson, 1994).

Alteration of gene expression in nitrogen uptake and assimilation pathways during polyphosphate accumulation

The role of arginine in neutralizing the negative charge of polyP is limited, at least during polyP overplus. Although arginine levels observed in the present study (100 – 140 nmol mg^{-1} DW, converted on the basis of dry weight) were comparable to that observed in *R. irregularis in vitro* culture (50 – 170 nmol mg^{-1} DW) (Jin *et al*., 2005), the levels were approximately an order of magnitude lower than those of polyP in terms of electric charge. Pi application, however, altered gene expression in the pathways for nitrogen assimilation and arginine biosynthesis/breakdown. The genes responsible for NO_3^- uptake (*NRT*) and subsequent reduction (*NAR* and *NIR*) were down-regulated in response to Pi application, and instead, the NH_4^+ permease gene *MEP* was up-regulated. This shift in nitrogen source from NO_3^- to NH_4^+ may contribute to alleviating accumulation of negative charge in the cell during massive accumulation of Pi. The up-regulation of the genes responsible for arginine biosynthesis/breakdown pathways in addition to V-type basic amino acid transport/export (*VBA/RTC*) suggests that *de novo* synthesis of arginine occurred during polyP accumulation, although no fluctuation in arginine level was detected. One interpretation is that newly synthesized arginine was translocated towards the plants (Govindarajulu *et al*., 2005), maintaining the cellular arginine levels. Although accumulation of basic amino acid in the vacuoles is likely to be metabolically independent from that of polyP in fungi (Cramer *et al.*, 1980; Dürr *et al.*, 1979), polyP accumulation may increase buffering capacity of the vacuoles for cationic compounds such as arginine, which would consequently activate the biosynthesis

and translocation of arginine.

Conclusion

The present study demonstrated the cellular responses of an AM fungus to increased Pi availability, which is the initial process of nutrient delivery in the plant-fungal associations. PolyP overplus i.e. rapid and massive accumulation of polyP in Pi-starved mycelia was accompanied by near-synchronous and -equivalent uptake of Na^+, K^+, Ca^{2+}, and Mg^{2+}, and these cellular events were achieved by the orchestrated regulation of gene expression responsible for mineral uptake, Pi and nitrogen metabolisms, and maintenance of cellular homeostasis. Given that the host plant supplies more carbohydrate to a more efficient fungal partner in terms of Pi delivery, namely the 'fair trade' (Kiers *et al*., 2011), those that are capable of delivering larger amounts of Pi are likely to be more competitive, at least under P deficient conditions. In this context, the capabilities of Pi acquisition and translocation may be directly relevant to competitiveness of individual fungi. Therefore, our study has important implications not only in the physiology but also in the ecology of the fungi and, further, provides a new direction for understanding the mechanism underlying competitiveness of the fungi.

Acknowledgements

The PPK-over expressing *E. coli* was a kind gift from Dr. A. Kornberg (Stanford University, CA). *L. japonicus* MG-20 seeds were supplied through Frontier Science Research Center of the University of Miyazaki funded by National BioResource Project. This work was mainly conducted in the open research facility in NARO/HARC (YK, NH, KY, RO, and TE) and

supported by the Grant-in-Aid for Scientific Research (22380042) from the Japan Society for the Promotion of Science (TE), the Grant in Aid for Scientific Research on Innovative Areas (No. 22128001 and 22128006) from Ministry of Education, Culture, Sports, Science and Technology of Japan (MK), and the Programme for Promotion of Basic and Applied Researches for Innovations in Bio-oriented Industry (KS). We also thank the Functional Genomics Facility for Illumina sequencing and the Data Integration and Analysis Facility for computational resources at National Institute for Basic Biology.

Reference

Ault-Riché D, Fraley CD, Tzeng CM, Kornberg A. 1998. Novel assay reveals multiple pathways regulating stress-induced accumulations of inorganic polyphosphate in *Escherichia coli*. *Journal of Bacteriology* **180**: 1841-1847.

Bago B, Pfeffer P, Shachar-Hill Y. 2001. Could the urea cycle be translocating nitrogen in the arbuscular mycorrhizal symbiosis? *New Phytologist* **149**: 4-8.

Bañuelos MA, Sychrova H, Bleykasten-Grosshans C, Souciet JL, Potier S. 1998. The Nha1 antiporter of *Saccharomyces cerevisiae* mediates sodium and potassium efflux. *Microbiology* **144**: 2749-2758.

Benjamini Y, Hochberg Y. 1995. Controlling the false discovery rate: a practical and powerful approach to multiple testing. *Journal of the Royal Statistical Society*: *Series B*, *Methodological* **57**: 289-300.

Bücking H, Heyser W. 1999. Elemental composition and function of polyphosphates in ectomycorrhizal fungi - an X-ray microanalytical study. *Mycological Research* **103**: 31-39.

Bücking H, Shachar-Hill Y. 2005. Phosphate uptake, transport and transfer by the arbuscular mycorrhizal fungus *Glomus intraradices* is stimulated by increased carbohydrate availability. *New Phytologist* **165**: 899-912.

Bun-Ya M, Nishimura M, Harashima S, Oshima Y. 1991. The *PHO84* gene of *Saccharomyces cerevisiae* encodes an inorganic phosphate transporter. *Molecular and Cellular Biology* **11**: 3229-3238.

Bürkert B, Robson A. 1994. ^{65}Zn uptake in subterranean clover (*Trifolium subterraneum* L.) by 3 vesicular-arbuscular mycorrhizal fungi in a root-free sandy soil. *Soil Biology and Biochemistry* **26**: 1117-1124.

Cagnac O, Leterrier M, Yeager M, Blumwald E. 2007. Identification and characterization of Vnx1p, a novel type of vacuolar monovalent cation/H^+ antiporter of *Saccharomyces cerevisiae*. *Journal of Biological Chemistry* **282**: 24284-24293.

Collins JF, Bai LQ, Ghishan FK. 2004. The SLC20 family of proteins: dual functions as sodium-phosphate cotransporters and viral receptors. *Pflügers Archiv, European Journal of Physiology* **447**: 647-652.

Conesa A, Gotz S, Garcia-Gomez JM, Terol J, Talon M, Robles M. 2005. Blast2GO: a universal tool for annotation, visualization and analysis in functional genomics research. *Bioinformatics* **21**: 3674-3676.

Cramer CL, Davis RH. 1984. Polyphosphate-cation interaction in the amino acid-containing vacuole of *Neurospora crassa*. *Journal of Biological Chemistry* **259**: 5152-5157.

Cramer CL, Vaughn LE, Davis RH. 1980. Basic amino acids and inorganic polyphosphates in *Neurospora crassa*: independent regulation of vacuolar pools. *Journal of Bacteriology* **142**: 945-952.

Dick CF, Dos-Santos ALA, Majerowicz D, Gondim KC, Caruso-Neves C, Silva IV, Vieyra A, Meyer-Fernandes JR. 2012. Na^+-dependent and Na^+-independent

mechanisms for inorganic phosphate uptake in *Trypanosoma rangeli*. *Biochimica et Biophysica Acta, General Subjects* **1820**: 1001-1008.

Dürr M, Urech K, Boller T, Wiemken A, Schwencke J, Nagy M. 1979. Sequestration of arginine by polyphosphate in vacuoles of yeast (*Saccharomyces cerevisiae*). *Archives of Microbiology* **121**: 169-175.

Ezawa T, Cavagnaro TR, Smith SE, Smith FA, Ohtomo R. 2003. Rapid accumulation of polyphosphate in extraradical hyphae of an arbuscular mycorrhizal fungus as revealed by histochemistry and a polyphosphate kinase/luciferase system. *New Phytologist* **161**: 387-392.

Ezawa T, Smith SE, Smith FA. 2001. Differentiation of polyphosphate metabolism between the extra- and intraradical hyphae of arbuscular mycorrhizal fungi. *New Phytologist* **149**: 555-563.

Ezawa T, Smith SE, Smith FA. 2002. P metabolism and transport in AM fungi. *Plant and Soil* **244**: 221-230.

Fiorilli V, Lanfranco L, Bonfante P. 2013. The expression of *GintPT*, the phosphate transporter of *Rhizophagus irregularis*, depends on the symbiotic status and phosphate availability. *Planta* **237**: 1267-1277.

Giri B, Mukerji K. 2004. Mycorrhizal inoculant alleviates salt stress in *Sesbania aegyptiaca* and *Sesbania grandiflora* under field conditions: evidence for reduced sodium and improved magnesium uptake. *Mycorrhiza* **14**: 307-312

Govindarajulu M, Pfeffer PE, Jin HR, Abubaker J, Douds DD, Allen JW, Bücking H, Lammers PJ, Shachar-Hill Y. 2005. Nitrogen transfer in the arbuscular mycorrhizal symbiosis. *Nature* **435**: 819-823.

Grabherr MG, Haas BJ, Yassour M, Levin JZ, Thompson DA, Amit I, Adiconis X, Fan L, Raychowdhury R, Zeng Q *et al.* 2011. Full-length transcriptome assembly from RNA-Seq data without a reference genome. *Nature Biotechnology* **29**: 644-652.

Harold FM. 1966. Inorganic polyphosphates in biology: structure, metabolism, and function. *Bacteriological Reviews* **30**: 772-794.

Harrison MJ, Vanbuuren ML. 1995. A phosphate transporter from the mycorrhizal fungus *Glomus versiforme*. *Nature* **378**: 626-629.

Hijikata N, Murase M, Tani C, Ohtomo R, Osaki M, Ezawa T. 2010. Polyphosphate has a central role in the rapid and massive accumulation of phosphorus in extraradical mycelium of an arbuscular mycorrhizal fungus. *New Phytologist* **186**: 285-289.

Hothorn M, Neumann H, Lenherr ED, Wehner M, Rybin V, Hassa PO, Uttenweiler A, Reinhardt M, Schmidt A, Seiler J *et al.* 2009. Catalytic core of a membrane associated eukaryotic polyphosphate polymerase. *Science* **324**: 513-516.

Huang RS, Smith WK, Yost RS. 1985. Influence of vesicular-arbuscular mycorrhiza on growth, water relations, and leaf orientation in *Leucaena leucocephala* (Lam.) de Wit. *New Phytologist* **99**: 229-243.

Hüerlimann BC, Stadler-Waibel M, Werner TP, Freimoser FM. 2007. Pho91 is a vacuolar phosphate transporter that regulates phosphate and polyphosphate metabolism in *Saccharomyces cerevisiae*. *Molecular Biology of the Cell* **18**: 4438-4445.

Jin H, Pfeffer PE, Douds DD, Piotrowski E, Lammers PJ, Shachar-Hill Y. 2005. The uptake, metabolism, transport and transfer of nitrogen in an arbuscular mycorrhizal symbiosis. *New Phytologist* **168**: 687-696.

Johansen A, Finlay RD, Olsson PA. 1996. Nitrogen metabolism of external hyphae of the arbuscular mycorrhizal fungus *Glomus intraradices*. *New Phytologist* **133**: 705-712.

Kiers ET, Duhamel M, Beesetty Y, Mensah JA, Franken O, Verbruggen E, Fellbaum CR, Kowalchuk GA, Hart MM, Bago A *et al.* 2011. Reciprocal rewards stabilize cooperation in the mycorrhizal symbiosis. *Science* **333**: 880-882.

Kornberg A, Rao NN, Ault-Riche D. 1999. Inorganic polyphosphate: a molecule of many functions. *Annual Review of Biochemistry* **68**: 89-125.

Kumble KD, Kornberg A. 1996. Endopolyphosphatases for long chain inorganic polyphosphate in yeast and mammals. *Journal of Biological Chemistry* **271**: 27146-27151.

Lawson JE, Douglas MG. 1988. Separate genes encode functionally equivalent ADP/ATP carrier proteins in *Saccharomyces cerevisiae*. Isolation and analysis of *AAC2*. *Journal of Biological Chemistry* **263**: 14812-14818.

Li H, Durbin R. 2010. Fast and accurate long-read alignment with Burrows-Wheeler transform. *Bioinformatics* **26**: 589-595.

Li H, Handsaker B, Wysoker A, Fennell T, Ruan J, Homer N, Marth G, Abecasis G, Durbin R. 2009. The Sequence Alignment/Map (SAM) format and SAMtools. *Bioinformatics* **25**: 2078-2079.

Li W, Godzik A. 2006. Cd-hit: a fast program for clustering and comparing large sets of protein or nucleotide sequences. *Bioinformatics* **22**: 1658-1659.

Li XL, Marschner H, George E. 1991. Acquisition of phosphorus and copper by VA-mycorrhizal hyphae and root-to-shoot transport in white clover. *Plant and Soil* **136**: 49-57.

Macdonald JC, Mazurek M. 1987. Phosphorus magnetic-resonance spectra of open-chain linear polyphosphates. *Journal of Magnetic Resonance* **72**: 48-60.

Maldonado-Mendoza IE, Dewbre GR, Harrison MJ. 2001. A phosphate transporter gene from the extra-radical mycelium of an arbuscular mycorrhizal fungus *Glomus*

intraradices is regulated in response to phosphate in the environment. *Molecular Plant-Microbe Interactions* **14**: 1140-1148.

Martinez P, Persson BL. 1998. Identification, cloning and characterization of a derepressible Na^+-coupled phosphate transporter in *Saccharomyces cerevisiae*. *Molecular and General Genetics* **258**: 628-638.

Olsson PA, Hammer EC, Wallander H, Pallon J. 2008. Phosphorus availability influences elemental uptake in the mycorrhizal fungus *Glomus intraradices*, as revealed by particle-induced X-ray emission analysis. *Applied and Environmental Microbiology* **74**: 4144-4148.

Robinson MD, McCarthy DJ, Smyth GK. 2010. edgeR: a Bioconductor package for differential expression analysis of digital gene expression data. *Bioinformatics* **26**: 139-140.

Smith SE, Read DJ. 2008. *Mycorrhizal symbiosis*: San Diego, CA, USA, Academic Press.

Sun JQ, Nishiyama T, Shimizu K, Kadota K. 2013. TCC: an R package for comparing tag count data with robust normalization strategies. *BMC Bioinformatics* **14**: 219.

Tani C, Ohtomo R, Osaki M, Kuga Y, Ezawa T. 2009. ATP-dependent but proton gradient-independent polyphosphate-synthesizing activity in extraradical hyphae of an arbuscular mycorrhizal fungus. *Applied and Environmental Microbiology* **75**: 7044-7050.

Tian CY, Feng G, Li XL, Zhang FS. 2004. Different effects of arbuscular mycorrhizal fungal isolates from saline or non-saline soil on salinity tolerance of plants. *Applied soil ecology* **26**: 143-148.

Tibbett M. 2000. Roots, foraging and the exploitation of soil nutrient patches: the role of mycorrhizal symbiosis. *Functional Ecology* **14**: 397-399.

Tisserant E, Kohler A, Dozolme-Seddas P, Balestrini R, Benabdellah K, Colard A, Croll D, Da Silva C, Gomez SK, Koul R *et al.* 2012. The transcriptome of the arbuscular mycorrhizal fungus *Glomus intraradices* (DAOM 197198) reveals functional tradeoffs in an obligate symbiont. *New Phytologist* **193**: 755-769.

Tisserant E, Malbreil M, Kuo A, Kohler A, Symeonidi A, Balestrini R, Charron P, Duensing N, Frei dit Frey N, Gianinazzi-Pearson V *et al.* 2013. Genome of an arbuscular mycorrhizal fungus provides insight into the oldest plant symbiosis. *Proceedings of the National Academy of Sciences* **110**: 20117-20122.

Versaw WK, Metzenberg RL. 1995. Repressible cation-phosphate symporters in *Neurospora crassa*. *Proceedings of the National Academy of Sciences of the United States of America* **92**: 3884-3887.

Viereck N, Hansen PE, Jakobsen I. 2004. Phosphate pool dynamics in the arbuscular mycorrhizal fungus *Glomus intraradices* studied by *in vivo* ^{31}P NMR spectroscopy. *New Phytologist* **162**: 783-794.

Zvyagilskaya R, Persson BL. 2003. Dual regulation of proton- and sodium-coupled phosphate transport systems in the *Yarrowia lipolytica* yeast by extracellular phosphate and pH. *IUBMB Life* **55**: 151-154.

Zvyagilskaya RA, Lundh F, Samyn D, Pattison-Granberg J, Mouillon J-M, Popova Y, Thevelein JM, Persson BL. 2008. Characterization of the Pho89 phosphate transporter by functional hyperexpression in *Saccharomyces cerevisiae*. *FEMS Yeast Research* **8**: 685-696.

Figures

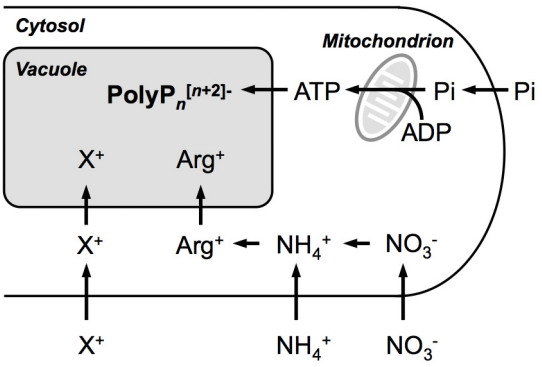

Fig. 1 Hypothetical transport and metabolic processes responsible for polyphosphate accumulation in extraradical mycelia of arbuscular mycorrhizal fungi. Phosphate (Pi) taken up into the cytosol is incorporated into ATP in mitochondria and then accumulated in the vacuoles as polyphosphate. A polyphosphate molecule consisting of *n*Pi-residues (polyP$_n$) possesses [n + 2] negative charge that should be neutralized by positively charged molecules such as inorganic cations (X^+) and arginine (Arg^+).

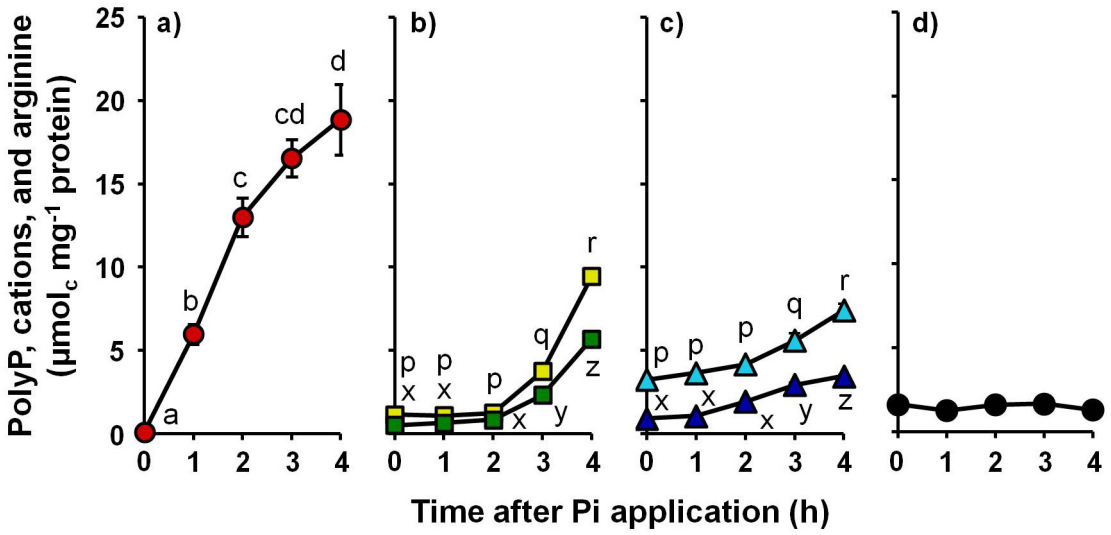

Fig. 2 Dynamics of cationic components during polyphosphate accumulation in extraradical mycelia of *Rhizophagus* sp. HR1 from 0 to 4 h after phosphate application: **a**, polyphosphate; **b**, monovalent cations Na^+ (yellow squares) and K^+ (green squares); **c**, divalent cations Ca^{2+} (light blue triangles) and Mg^{2+} (dark blue triangles); **d**, arginine. One mM phosphate solution was applied to the hyphal compartment of mesh bag culture system, and then extraradical mycelia were harvested from the compartment at 1 h intervals. The levels are expressed as electric charge mol per unit protein. Vertical bars are ± SE (n = 3). Different letters indicate significant difference at $P < 0.05$ (Tukey-Kramer test).

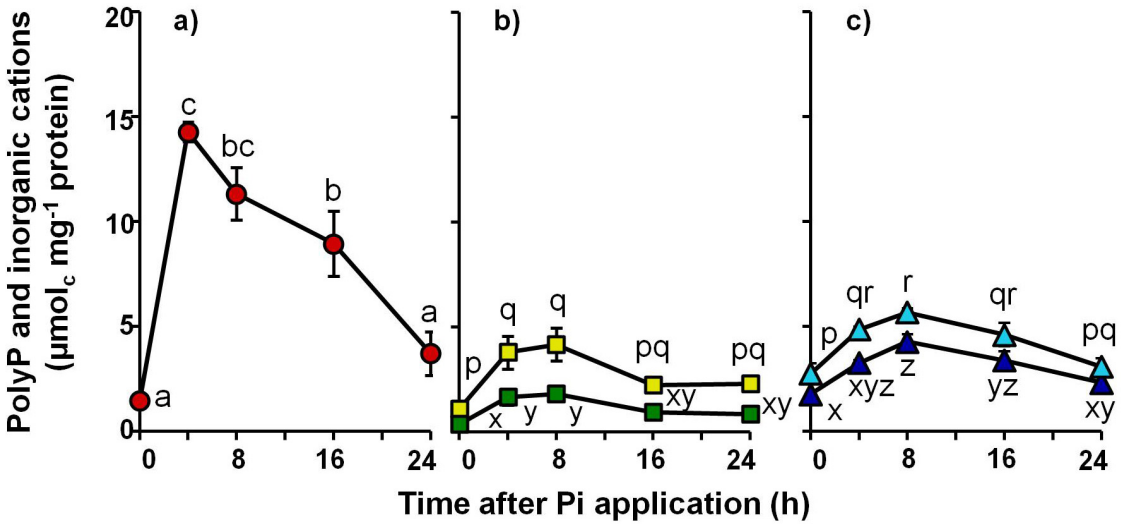

Fig. 3 Dynamics of inorganic cations during polyphosphate accumulation in extraradical mycelia of *Rhizophagus* sp. HR1 from 0 to 24 h after phosphate application: **a**, polyphosphate; **b**, monovalent cations Na^+ (yellow squares) and K^+ (green squares); **c**, divalent cations Ca^{2+} (light blue triangles) and Mg^{2+} (dark blue triangles). One mM phosphate solution was applied to the hyphal compartment of mesh bag culture system, and then extraradical mycelia were harvested from the compartment at 4 and 8 h intervals. The levels are expressed as electric charge mol per unit protein. Vertical bars are ± SE (n = 3). Different letters indicate significant difference at $P < 0.05$ (Tukey-Kramer test).

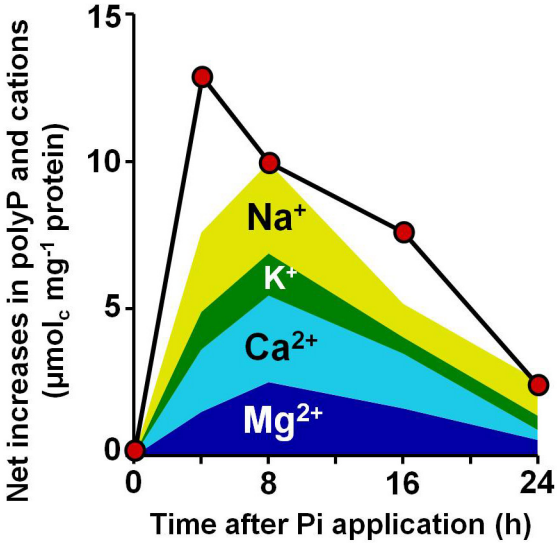

Fig. 4 Near-synchronous and -equivalent changes in total electric charge of Na^+, K^+, Ca^{2+}, and Mg^{2+} (shown as a stacked area chart) with that of polyphosphate (polyP) (red circles) in extraradical mycelia of *Rhizophagus* sp. HR1. The data in Fig. 3 were used to calculate net changes in the levels from time zero.

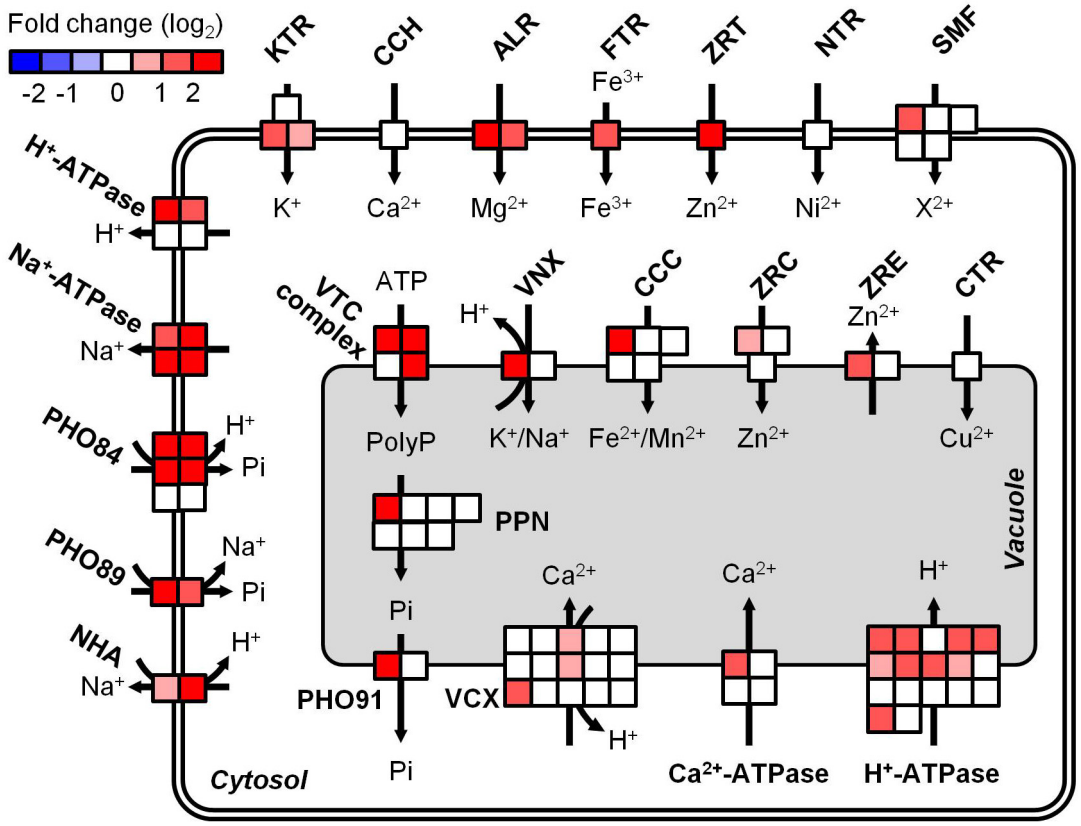

Fig. 5 Expression profile of genes responsible for phosphate/cation uptake in extraradical mycelia of *Rhizophagus* sp. HR1 during polyphosphate accumulation. Each square indicates a representative gene that possesses the longest ORF among a group of putative protein-coding genes clustered based on ≥ 95% sequence similarities, and genes that are predicted to encode the same functional protein are grouped. Significant fold-changes ($\log_2$) from 0 to 4 h after Pi application were indicated in red (up-regulated) and blue (down-regulated) colors. Statistical test was performed using edgeR package in R coupled with iDEGES/edgeR normalization (false discovery rate < 0.05; n = 3). Abbreviations for gene products are: ALR, Mg^{2+} transporter; CCC, vacuolar Fe^{2+}/Mn^{2+} transporter; CCH, Ca^{2+} channel; CTR, copper transporter; FTR, Fe^{3+} permease; KTR, K^+ transporter; NHA, Na^+/H^+ antiporter; NTR, Ni^{2+}

transporter; PHO84, H^+/Pi symporter; PHO89, Na^+/Pi symporter; PHO91, vacuolar Pi transporter; PPN, endopolyphosphatase; SMF, divalent metal ion transporter; VCX, vacuolar Ca^{2+}/H^+ antiporter; VNX, vacuolar monovalent cation/H^+ antiporter; VTC complex, vacuolar transporter chaperone complex; ZRC, vacuolar Zn^{2+} transporter; ZRE, vacuolar Zn^{2+} exporter; ZRT, Zn^{2+} transporter.

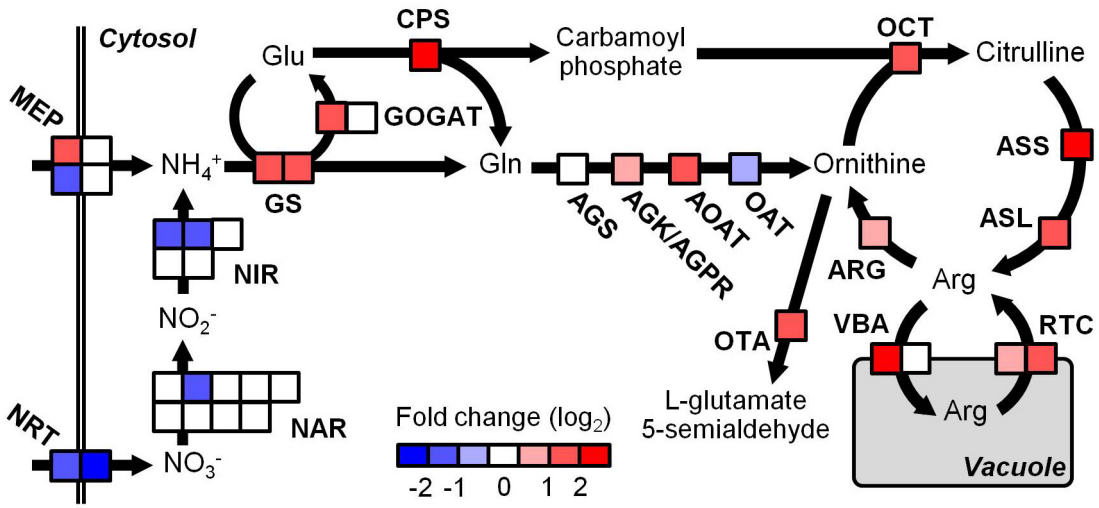

Fig. 6 Expression profile of genes responsible for nitrogen assimilation and arginine biosynthesis in extraradical mycelia of *Rhizophagus* sp. HR1 during polyphosphate accumulation. Each square indicates a representative gene that possesses the longest ORF among a group of putative protein-coding genes clustered based on ≥ 95% sequence similarities, and genes that are predicted to encode the same functional protein are grouped. Significant fold changes (log_2) from 0 to 4 h after Pi application were indicated in red (up-regulated) and blue (down-regulate). Statistical test was performed using edgeR package in R coupled with iDEGES/edgeR normalization (false discovery rate < 0.05; n = 3). Abbreviations for gene products are: AGK/AGPR, acetylglutamate kinase and N-acetyl-γ-glutamyl-phosphate reductase; AGS, acetylglutamate synthase; AOAT, acetylornithine aminotransferase; ARG, arginase; ASL, argininosuccinate lyase; ASS, argininosuccinate synthetase; CPS, carbamoyl phosphate synthetase; GOGAT, glutamate synthase; GS, glutamine synthetase; MEP, NH_4^+ permease; NAR, nitrate reductase; NIR, nitrite reductase; NRT, nitrate transporter; OAT, ornithine acetyltransferase; OCT, ornithine carbamoyltransferase; OTA, ornithine transaminase; RTC, vacuolar membrane transporter for cationic amino acids; VBA, permease of basic amino acids in the vacuolar membrane.

Supporting Information

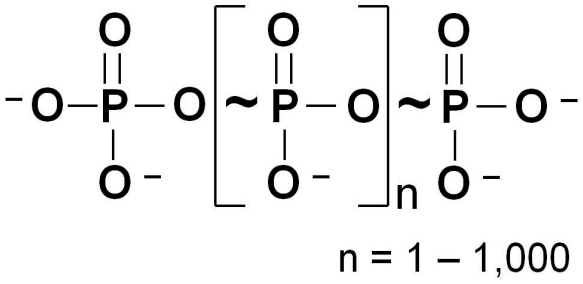

Fig. S1 Structural formula of polyphosphate. Polyphosphate is a linear chain of phosphate linked by high-energy phosphoanhydride bonds. Fully dissociated polyphosphate has one negative charge per residue in addition to two extra charges of the terminal residues.

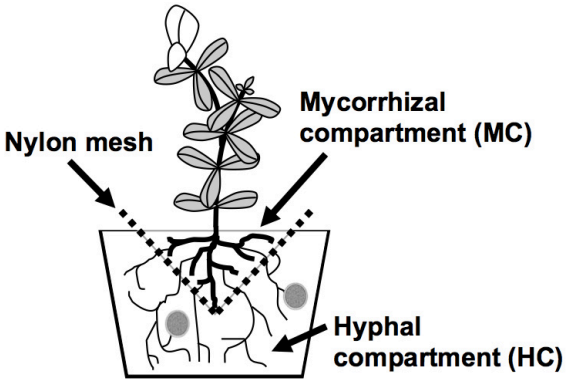

Fig. S2 Mesh bag culture system. The mycorrhizal (MC) and hyphal (HC) compartments were separated by a cone-shaped 37-mm nylon mesh bag. The pore size of the nylon mesh was small enough to prevent plant roots from passing but large enough to allow AM fungal hyphae to pass through. The media in the MC and HC were autoclaved river sand with particle size distributions of 0.1 – 3 mm and 1 – 3 mm, respectively.

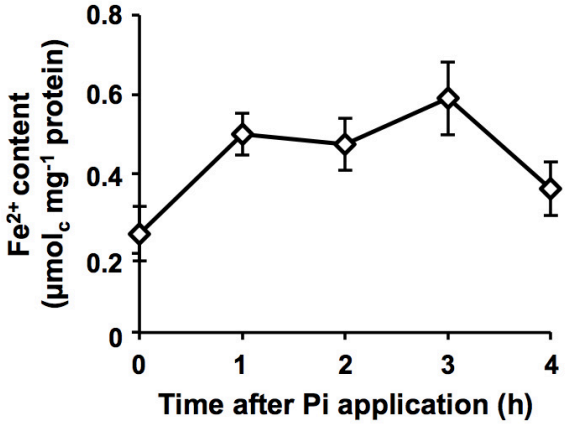

Fig. S3 Dynamics of Fe^{2+} during polyphosphate accumulation in extraradical mycelia of *Rhizophagus* sp. HR1 grown in the mesh bag compartment system. One mM phosphate solution was applied at zero time, and then extraradical mycelia were harvested from the hyphal compartment at 1 h intervals. The levels are expressed as electric charge mol per unit protein. Vertical bars are SE (n = 3). No significant difference in the level was observed among all time points ($P > 0.05$).

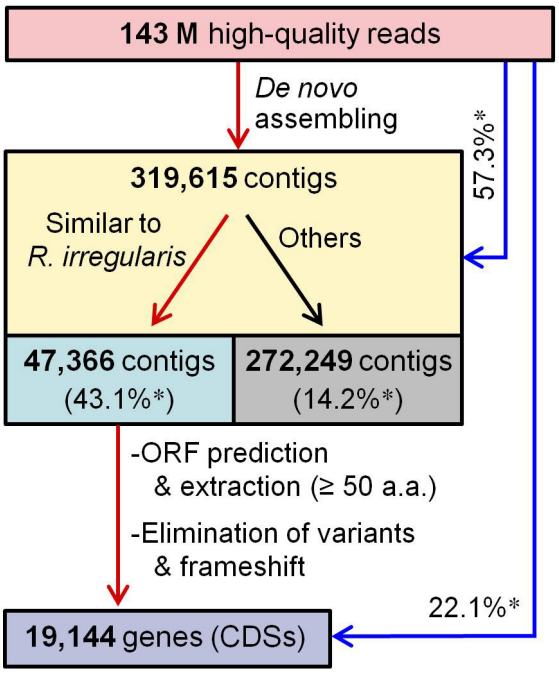

Fig. S4 Workflow for gene prediction in the RNA-Seq of *Rhizophagus* sp. HR1 transcriptome. Contigs obtained by *de novo* assembly of high-quality Illumina reads were subjected to BLASTN searches to select those originated from *Rhizophagus* sp. HR1 based on similarity to the sequences in *R. irregularis* genome database, and ORFs of 50 or longer amino acid residues were predicted and extracted from the contigs. *Percentage of reads mapped to the contigs/CDSs.

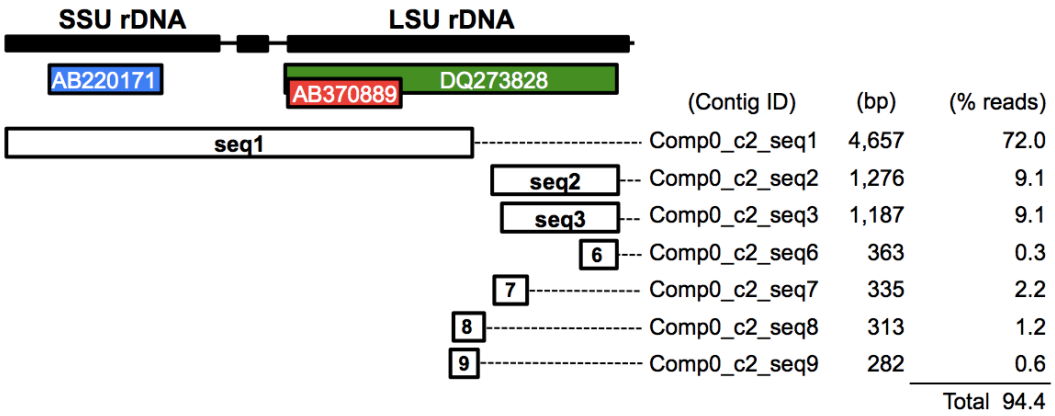

Fig. S5 Alignment of ribosomal RNA gene (rDNA) of *Rhizophagus* sp. HR1 and contigs obtained in RNA-Seq. Seven contigs originated from the comp0_c2 locus (seq1 – seq3, seq6 – seq9) showed the highest similarity to *Rhizophagus* sp. HR1 small-subunit (SSU) rDNA (AB220171), large-subunit (LSU) rDNA (AB370889), and *R. irregularis* LSU rDNA (DQ273828). Of all the reads mapped to rRNA genes of various organisms, 94.4% were mapped to these 7 contigs. Note that AB370889 and DQ273828 showed 95.0% similarity.

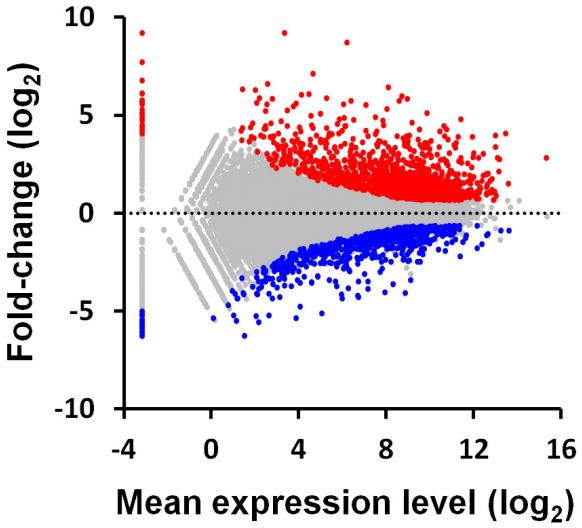

Fig. S6 Fold-change (log_2) in expression level of genes in extraradical mycelia of *Rhizophagus* sp. HR1 from 0 to 4 h after phosphate application with respect to mean expression levels (log_2). Red and blue dots represent significantly up-regulated and down-regulated genes, respectively, in response to Pi application. Statistical test was performed using edgeR package in R coupled with iDEGES/edgeR normalization (false discovery rate < 0.05; $n = 3$).

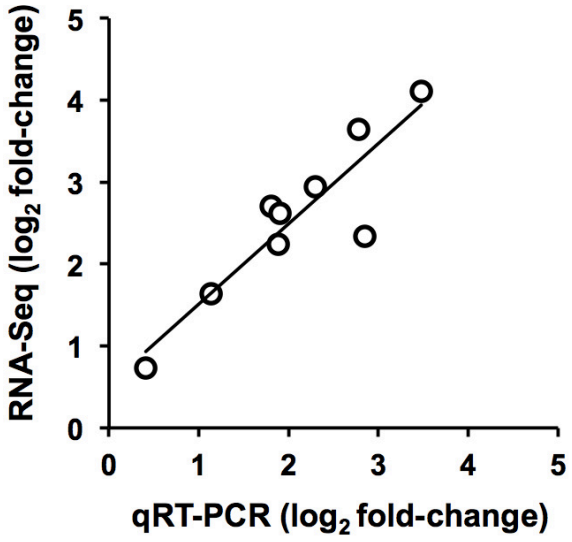

Fig. S7 Validation of RNA-Seq data by quantitative RT-PCR (qRT-PCR). Fold-changes (log_2) in expression level of the genes from 0 to 4 h after phosphate application revealed by RNA-Seq are plotted against those revealed by qRT-PCR. The Pearson correlation coefficient is 0.906 ($P < 0.001$, $n = 3$). The names of gene products and their ORF IDs (in parentheses) employed in this analysis are as follows: H^+/Pi symporter (Rh7140 and Rh78270), Na^+/Pi symporter (Rh99477 and Rh80369), vacuolar transporter chaperone 1 (Rh89101) and 4 (Rh2668), Na^+/H^+ antiporter NHA (Rh147608 and Rh80375), and vacuolar monovalent cation/H^+ antiporter VNX (Rh5707).

Table S1 Target genes and primers in quantitative RT-PCR.

ORF ID		Putative function	Forward primer/ reverse primer
h7140	R	H^+/Pi symporter	CCGCTGTTGATTACTGTTGG/ CGGAATTGTGAGACGGAAG
h78270	R	H^+/Pi symporter	GGAAAACTTGGAGCTATCGTTG/ CCACCAATAAACATCCATGCTG
h99477	R	Na^+/Pi symporter	CGTGGTTTAATCGCTGTGC/ CGTTATACCCACGGTAACAGATG
h80369	R	Na^+/Pi symporter	CGACCCATTGCATTACAGG/ GCCCAACTAAAGAAGCACCA
h89101	R	Subunit 1 of vacuolar transporter chaperon complex (VTC1)	GCTATCATGCTCTACGCTCTGTC/ GGAAAATGCAGAGCACAGTTGG
h2668	R	Subunit 4 of vacuolar transporter chaperon complex (VTC4)	ACTGGCGTCGAATGGATATTG/ AACCCATACTGGTGGCTCTTG
h147608	R	H^+/Na^+ antiporter in the plasma membrane (NHA)	TCGTTGACAGGAGGAACAATC/ GGCATTTCTTCATTAGGTGGTG
h80375	R	H^+/Na^+ antiporter in the plasma membrane (NHA)	CTCTTATTTCGTCGCCTTCCTATC/ GCAGCTACTCCAATAGGTCCAAA
h5707	R	H^+/monovalent cation antiporter in the vacuolar membrane (VNX)	CACATGAACATTCGGAACGAC/ GATGCTGTTGTGGGTGCAG
h122513	R	α-Tubulin	GCTTGTTGTTTGTTGTATCGTG/ TGAATGGTACGTTTGGTCTTG

Table S2 Dynamics of free amino acids during polyphosphate accumulation in extraradical mycelia of *Rhizophagus* sp. HR1 after phosphate application.

	Time after Pi application (h)									
	0		1		2		3		4	
	(nmol mg^{-1} protein)									
Arginine	1634	± 379	1277	± 277	1627	± 235	1671	± 146	1320	± 120
Asparagine	447	± 63	345	± 65	387	± 49	361	± 52	290	± 22
Glutamic acid	163	± 19 a	112	± 12 b	91	± 4 b	91	± 4 b	76	± 7 b
Alanine	103	± 5 a	91	± 6 ab	85	± 4 ab	75	± 3 bc	59	± 5 c
Urea	71	± 21	62	± 5	65	± 5	67	± 7	66	± 13
Serine	66	± 8	56	± 6	59	± 4	51	± 1	50	± 7
Glutamine	62	± 3 a	39	± 2 b	34	± 2 bc	35	± 1 bc	28	± 2 bc
Lysine	61	± 11	58	± 7	56	± 8	53	± 5	46	± 3
Ornithine	58	± 30	30	± 3	36	± 3	31	± 1	31	± 2
Isoleucine	52	± 8	45	± 5	43	± 4	36	± 2	33	± 4
Glycine	50	± 4	43	± 5	44	± 3	43	± 2	39	± 6
Aspartic acid	44	± 6	34	± 3	34	± 1	33	± 2	30	± 2
Valine	43	± 7 a	33	± 4 ab	35	± 3 ab	25	± 1 ab	23	± 3 b
Threonine	41	± 7 a	30	± 4 ab	30	± 3 ab	24	± 2 ab	20	± 2 b
NH_3	30	± 4	31	± 4	30	± 2	30	± 1	32	± 3
Leucine	29	± 4	34	± 7	30	± 5	27	± 4	25	± 3
Tyrosine	25	± 4	24	± 3	22	± 3	19	± 2	16	± 1
Proline	18	± 2	16	± 2	15	± 2	18	± 1	15	± 1
Histidine	15	± 2	17	± 2	17	± 2	19	± 1	16	± 1
Cysteine	12	± 2	10	± 1	11	± 1	12	± 1	10	± 1
Phenylalanine	8	± 2	10	± 3	9	± 2	9	± 1	8	± 1
Methionine	1	± 1	n.d.		1	± 1	2	± 1	1	± 1
Tryptophan	n.d.		n.d.		n.d.		n.d.		n.d.	
Total	3050	± 524	2420	± 329	2782	± 244	2745	± 183	2248	± 138

Mean ± SE (n = 3). Different letters indicate significant difference among the time points at $P < 0.05$ (Turkey-Kramer Test). n.d., not detected.

Tables S3-S10 are in a separate Excel file that could be ordered through email to the corresponding author.